

Dependence of magnetic properties on micro- to nanostructure of CoNiFe films

Fernando M. F. Rhen^{a)} and Saibal Roy
 Tyndall National Institute, University College Cork, Cork, Ireland

(Received 9 October 2007; accepted 3 March 2008; published online 16 May 2008)

The magnetic properties of electrodeposited CoNiFe films with thicknesses varying from 0.20 to 10 μm were studied. The films show a single face-centered-cubic CoNiFe phase with grain sizes ranging from 23 to 29 nm. The coercivity is controlled by a combination of the morphology and nanocrystalline structure of the deposits. The nanocrystalline grain size determines the intrinsic coercivity associated with crystalline anisotropy as in the random anisotropy model, whereas an additional morphology term of coercivity is controlled by the thickness inhomogeneity on a submicron scale. The thin films show considerable roughness and a higher coercivity, up to a level of 560 A m^{-1} (7.0 Oe) in 250 nm films. The thick films show coercivity values of as low as 16 A m^{-1} (0.2 Oe). The coercivity dependence on thickness was fitted using a simple model combining a morphology dependent additional contribution term to the random anisotropy model as $H_c = H_c^{\text{morph}} + H_c^{\text{anis}}$. Good agreement between the model and the experimental results was obtained.
 © 2008 American Institute of Physics. [DOI: 10.1063/1.2919059]

I. INTRODUCTION

The development of electrodeposited soft magnetic films has been motivated by applications in recording media as read/write heads^{1,2} and microelectromechanical systems (MEMS).^{3,4} Permalloy has been widely used in recording heads² and MEMS applications^{3,4} with a magnetic saturation of 1 T and a low coercivity of $<40 \text{ A m}^{-1}$ (0.5 Oe). However, there is a need for softer materials with higher saturation magnetization as the information density in hard disk drives^{1,2} increases and better performance associated with miniaturization is expected in MEMS devices.³ A variety of CoNiFe and CoFe-based alloys, including CoNiFe,⁴⁻⁹ CoNiFeS,¹⁰ CoFeSnP,¹¹ CoFeCu,² CoFeB,¹² and CoFeP,¹¹ has been studied. Among them, the electroplated CoNiFe alloy appears as a promising candidate due to its high saturation magnetization ($\mu_0 M_s \sim 2.0\text{--}2.1 \text{ T}$) and low coercivity field, 95–160 A m^{-1} (1.2–2 Oe).^{1,13,14}

Several approaches have been employed to prepare soft CoNiFe, including the addition of inorganic and organic additives and control of the plating conditions. Some additives are employed to increase resistivity by incorporating S,^{15,16} C,^{17,18} and B.¹⁹ Other additives are used to reduce stress and improve the appearance of the film. Deposits obtained from electrolytes containing additives are reported to decrease the saturation magnetization and increase the coercivity.¹⁵⁻¹⁸ The reported saturation magnetization from electrolytes with additives ranged from 1.5 to 1.9 T. The lowest in-plane coercivity in electrodeposited CoNiFe alloys is obtained in additive-free electrolytes, which is associated with a nanocrystalline structure where body-centered-cubic (bcc) and face-centered-cubic (fcc) CoNiFe phases coexist with grain sizes between 10 and 20 nm.^{1,7} Therefore, in light of the current literature, films outside of the bcc/fcc phase boundary

are expected to show a larger grain size and thereby a higher coercivity. Here, we show that electrodeposited CoNiFe films with a single fcc phase can be obtained with a small grain size, and a very low in-plane coercivity is achieved. Furthermore, we correlated the coercivity with the microstructure of the deposits.

II. EXPERIMENTAL SETUP

The electrolytic bath for the preparation of CoNiFe films is similar to that employed by Osaka *et al.*¹ Deposition was carried out in a 50 mL vessel, with mechanical agitation, in an open atmosphere, and using the galvanic pulse reverse plating technique as described elsewhere.²⁰ Electrodes were cut out from commercial brass and coated with a polymer, which left a plating area of $5 \times 5 \text{ mm}^2$. The microstructure, composition, thickness, magnetic properties, and crystalline structure were determined using scanning electron microscopy, energy-dispersive x-ray spectroscopy (EDX), a surface profilometer, a 5 T superconducting quantum interference device magnetometer, and x-ray diffraction with Cu $K\alpha$ radiation, respectively. Films of different thicknesses (0.20–10 μm) were obtained by varying the deposition time.

III. RESULTS AND DISCUSSION

X-rays diffractograms of electrodeposited CoNiFe with different thicknesses reveal the same crystallographic structure, independent of the thickness of the films, as shown in Fig. 1. The grain size was calculated by using the Debye-Scherrer formula and the full width at half maximum, we obtain values ranging from 23 to 29 nm. We identify the main peak at 44.3° as (111) fcc CoNiFe, which is in accordance with the literature.⁷ Magnetic measurements and EDX analysis show that the magnetization saturation and composition are also thickness independent, with values of 1.9 T

^{a)}Electronic mail: Fernando.rhen@tyndall.ie.

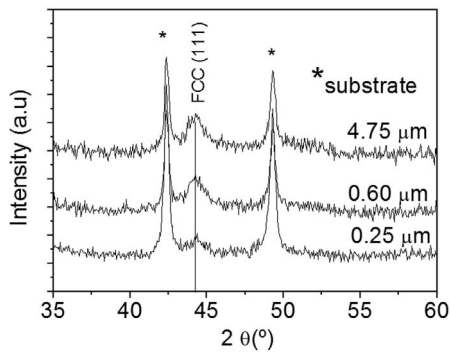


FIG. 1. Diffraction pattern of electrodeposited CoNiFe with different thicknesses. The magnetic phase present is fcc CoNiFe.

and $\text{Co}_{66.7}\text{Ni}_{16.8}\text{Fe}_{16.5}$, respectively. Room temperature hysteresis loops for films with various thicknesses are shown in Fig. 2. To rule out the possibility of the effect of inhomogeneous composition on coercivity due to initial growth, we have polymer coated a free-standing $9.5 \mu\text{m}$ film on one side and etched down to $1\text{--}2 \mu\text{m}$ from the initial plating side, thereby eliminating the initially deposited layers. We measured the coercivity before and after wet etching and obtained 16 and 102 A m^{-1} , respectively. The films became

rough and lost their mirrorlike appearance after wet etching. This confirms that roughness is mainly responsible for the higher coercivity observed in thin CoNiFe deposits.

The magnetization (M) depends on the internal field (H_{int}), which can be calculated from:

$$H_{\text{int}} = H_{\text{ext}} - DM, \quad (1)$$

where D is the demagnetizing factor and H_{ext} is the external applied field. The demagnetizing factor for a thin film is ~ 0 for in plane and ~ 1 for out of plane.²¹ For a magnetic field applied along the hard axis, $M = \mu_r H_{\text{int}}$; thereby Eq. (1) reduces to $M = \gamma H_{\text{ext}}$, where γ is $(D + 1/\mu_r)^{-1}$ and μ_r is the relative permeability. In out-of-plane measurements (Fig. 2), the linear dependence of magnetization on H_{ext} for a sample with a thickness of up to $1.47 \mu\text{m}$ indicates that the anisotropy is mainly in plane. This is in contrast to the $4.75 \mu\text{m}$ thick film, where there is an out-of-plane contribution to anisotropy, which is also consistent with the fact that the in-plane hard and easy axis coercivities converge to the same value as the film thickness is increased (Fig. 3).

According to the random anisotropy model,^{22,23} the coercivity of a nanocrystalline material depends on the grain size:

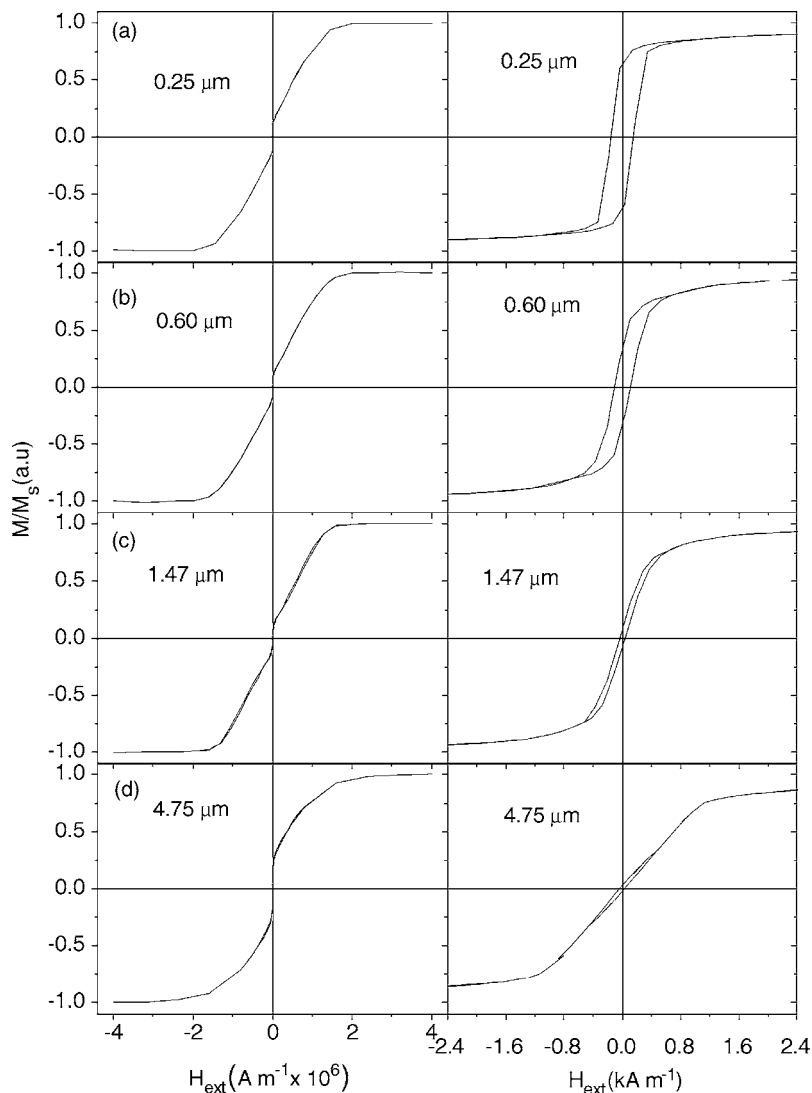


FIG. 2. Out-of-plane (left) and in-plane (right) room-temperature magnetization curves for electrodeposited CoNiFe with various thicknesses: (a) $0.25 \mu\text{m}$, (b) $0.60 \mu\text{m}$, (c) $1.47 \mu\text{m}$, and (d) $4.75 \mu\text{m}$.

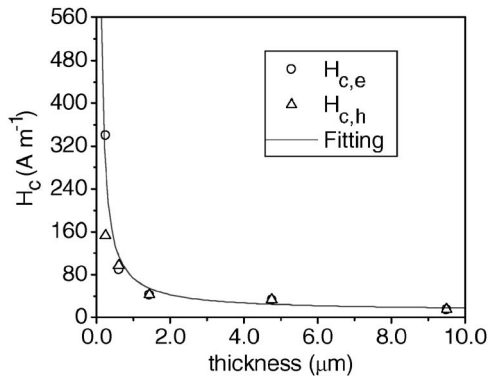


FIG. 3. Room-temperature coercivity dependence on the thickness of electroplated CoNiFe. Measured with the field in plane along the easy axis ($H_{c,e}$) and along the hard axis ($H_{c,h}$). The continuous line is a fit of Eq. (3) reduced to $H_{c,e}=60.6 \times 10^{-6}t^{-1}+12$.

$$H_c^{\text{anis}} \approx p_c K_1^4 D^6 / J_s A^3, \quad (2)$$

where p_c , K_1 , D , J_s , and A are the particle shape prefactor, the anisotropy constant, the grain size, the magnetization saturation, and the exchange constant, respectively. In this model the effective anisotropy is an average of the crystalline anisotropy within the exchange length (typically ~ 50 nm) and the coercivity is very sensitive to the grain size $H_c^{\text{anis}} \propto D^6$.

Recently, Zhao *et al.*²⁴ proposed a model to describe coercivity, which yields $H_c \propto 1/t$. This model includes the effect of roughness on the demagnetizing field and on domain-wall movement, which in turn is reflected on coercivity:

$$H_c^{\text{morph}} = (\rho_{\text{rms}}/J_s)[A\pi^2/D_w t + K_1 D_w/2t + (D_w t + 2D_w^2)\pi J_s^2/(t + D_w)^2]. \quad (3)$$

Here ρ_{rms} is a dimensionless measure of roughness,²⁴ A is the exchange constant, D_w is the domain-wall width, t is the film thickness, K_1 is the anisotropy constant, and J_s is the saturation magnetization. In this model the additional contribution to the coercivity becomes zero in a perfectly flat smooth film.

In an ideal case, combining the two contributions yields

$$H_c = H_c^{\text{morph}} + H_c^{\text{anis}}. \quad (4)$$

The anisotropy term of coercivity dominates in smooth thick films, whereas the roughness term dominates in thin films.

The behavior of the coercivity dependence on thickness (Fig. 3) can be understood in terms of the microstructure of the deposition. It can be noted that the micron-scale granular structure in thin films creates a rough surface [Figs. 4(a) and 4(b)]. In this structure the domain walls tend to be pinned due to a variation in thickness. Therefore, the variation in the thickness of the thin films results in an increase in coercivity. The roughness decreases [Figs. 4(c) and 4(d)] as the film thickness increases, and so it is easier for domain-wall movement, which is also reflected in the coercivity. We observed that the CoNiFe thick films are either smooth or have a roughness [Figs. 4(c) and 4(d)] that is small compared to the total thickness, and thereby exhibit lower coercivity (16 A m^{-1}). Furthermore, the observed coercivity can be understood also in terms of the film morphology and crystalline anisotropy according to Eq. (4). The morphology of the film is reflected in the inhomogeneity of the film thickness. The crystalline anisotropy controls the coercivity in smooth thick films and is represented in the random anisotropy model. Using $K_1 \sim 10^4 \text{ J m}^{-3}$, $D=2 \times 10^{-9} \text{ m}$, $A \sim 2 \times 10^{-11} \text{ J m}^{-1}$, $J_s=1.9 \text{ T}$, $p_c=0.64$ (cubic particle randomly oriented)²⁵ results in coercivities of the order of 10^1 A m^{-1} , which is in the same order of magnitude of the coercivity of thick films, 16 A m^{-1} . Since the grain sizes of CoNiFe are independent of film thickness, we conclude that thickness inhomogeneities control the coercivity in thin films.

The domain-wall width for most soft material materials is typically between 10 and 100 nm. Then, by using material parameters of $K_1 \sim 10^4 \text{ J m}^{-3}$, $D_w=10^{-7} \text{ m}$, $A \sim 2 \times 10^{-11} \text{ J m}^{-1}$, and $J_s=1.9 \text{ T}$ in Eq. (3) (neglecting the third term) and the fitting from the plot $H_{c,e}=60.6 \times 10^{-6}t^{-1}+12$ (Fig. 3), we obtain $\rho_{\text{rms}}=0.047$, which is of the same order of magnitude of values estimated from the micrograph in Fig. 4, i.e., 0.18. Neglecting the third term in Eq. (3) for calculation

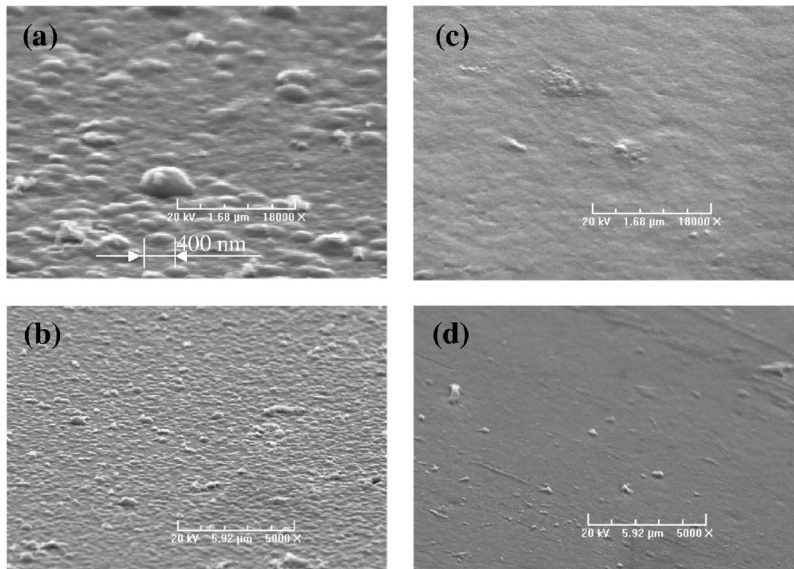


FIG. 4. Micrographs of electrodeposited material with thicknesses of (a), (b) $0.6 \mu\text{m}$ and (c), (d) $9.5 \mu\text{m}$. The pictures were taken with the sample's surface tilted 30° to the electron beam.

and fitting does not affect our analysis as it is a second-order correction. The estimate of $\rho_{\text{rms}} \sim (1/2.8)\delta/\gamma$ is obtained from Fig. 4 using a peak-to-peak roughness (δ) amplitude of 200 nm and a correlation length of 400 nm (γ). Therefore, qualitative agreement is obtained by using Zhao *et al.*'s model of coercivity²⁴ and our measurements of the thin films.

The rough structure of the thin film is inherited from the electrochemical process. Electrochemical deposition of a metal or metal alloy always starts from nucleation and then evolves into multidimensional growth. Therefore, at the first stage of electrodeposition, sites nucleate preferentially²⁰ on the electrode surface and the deposit starts to grow from each nucleated site, forming a granular structure. When the grains become large enough, percolation occurs. At this final stage uniform vertical growth may dominate and consequently roughness can be reduced. This is consistent with our microscopic observations of CoNiFe, suggesting that uniform vertical growth really did occur in thick films in the later stages of deposition.

IV. CONCLUSION

We have prepared electrodeposited CoNiFe and showed that low coercivity can be obtained in the fcc phase. Controlling the thickness of the films has a direct effect on the anisotropy direction, which in turn determines the coercivity of the deposits. Thin films are rough and show higher coercivities. On the other hand, thick smooth films exhibit coercivities as low as 16 A m^{-1} (0.2 Oe).

The dependence of the coercivity on thickness was correlated with the microstructure of the deposit, which is governed by the nucleation and growth during the electrochemical process. Thin films are rough, showing a granular structure, which contrasts to smooth thick films. Typically, the microstructure of thin films is granular with grain sizes in the range of 300–500 nm. The crystallite structure was identified as fcc CoNiFe with grain sizes ranging from 23 to 29 nm and it does not depend on thickness. The crystallite size determines the intrinsic coercivity of the films and roughness produces an additional contribution, which increases pinning and hence the coercivity of the deposits. We propose a simple model to represent coercivity, which combines the morphology and grain size contributions, hence covering nano- to microstructure contributions. We find good agree-

ment between our experimental results and the model. Thick CoNiFe with low coercivity may find application in magnetic MEMS and as a core material for energy conversion.

ACKNOWLEDGMENT

This work was supported by Enterprise Ireland under PEIG Magnetics and Science Foundation Ireland Principal Investigator (SFI-PI) Grant No. 06/IN.1/I98.

- ¹T. Osaka, M. Takai, K. Hayashi, K. Ohashi, M. Saito, and K. Yamada, *Nature (London)* **392**, 796 (1998).
- ²P. C. Andricacos and N. Robertson, *IBM J. Res. Develop.* **42**, 671 (1998).
- ³E. J. O'Sullivan, E. I. Cooper, L. T. Romankiw, K. T. Kwietniak, P. L. Trouilloud, J. Horkans, C. V. Jahnes, I. V. Babich, S. Krongelb, S. C. Hedge, J. A. Tornello, N. C. LaBianca, J. M. Cotte, and T. J. Chainer, *IBM J. Res. Develop.* **42**, 681 (1998).
- ⁴P. T. Tang, *Electrochim. Acta* **47**, 61 (2001).
- ⁵X. Liu, G. Zangari, and L. Shen, *J. Appl. Phys.* **87**, 5410 (2000).
- ⁶R. Chesnutt, *J. Appl. Phys.* **73**, 6223 (1993).
- ⁷X. Liu, G. Zangari, and M. Shamsuzzoha, *J. Electrochem. Soc.* **150**, C159 (2003).
- ⁸I. Tabakovic, V. Inturi, and S. Riemer, *J. Electrochem. Soc.* **149**, C18 (2002).
- ⁹K. Ohashi, Y. Yasue, M. Saito, K. Yamada, T. Osaka, M. Takai, and K. Hayashi, *IEEE Trans. Magn.* **34**, 1462 (1998).
- ¹⁰M. Takai, K. Hayashi, M. Aoyaki, and T. Osaka, *J. Electrochem. Soc.* **144**, L203 (1997).
- ¹¹K. Hironaka and S. Uedaira, *IEEE Trans. Magn.* **26**, 2421 (1990).
- ¹²S. H. Liao, U.S. Patent No. 5,168,410 (1992).
- ¹³I. Tabakovic, S. Riemer, V. Inturi, P. Jallen, and A. Thayer, *J. Electrochem. Soc.* **147**, 219 (2000).
- ¹⁴T. Osaka, M. Takai, Y. Sogawa, T. Momma, K. Ohashi, M. Saito, and K. Yamada, *J. Electrochem. Soc.* **146**, 2092 (1999).
- ¹⁵T. Osaka, M. Takai, Y. Sogawa, T. Momma, K. Ohashi, M. Saito, and K. Yamada, *J. Electrochem. Soc.* **146**, 2092 (1999).
- ¹⁶T. Osaka, T. Sawaguchi, F. Mizutani, T. Yokoshima, M. Takai, and Y. Okinaka, *J. Electrochem. Soc.* **146**, 3295 (1999).
- ¹⁷T. Osaka, T. Yokoshima, and T. Nakanishi, *IEEE Trans. Magn.* **37**, 1761 (2001).
- ¹⁸T. Yokoshima, M. Kaseda, M. Yamada, T. Nakanishi, T. Momma, and T. Osaka, *IEEE Trans. Magn.* **35**, 2499 (1999).
- ¹⁹T. Yokoshima, D. Kanedo, M. Akahori, H. S. Nam, and T. Osaka, *J. Electroanal. Chem.* **491**, 197 (2000).
- ²⁰S. Roy, A. Connell, M. Ludwig, N. Wang, T. O'Donnell, M. Brunet, P. McCloskey, C. O'Mathuna, A. Barman, and R. J. Hicken, *J. Magn. Mater.* **290-291**, 1524 (2005).
- ²¹D. C. Cronmeyer, *J. Appl. Phys.* **70**, 2911 (1991); J. A. Osborn, *Phys. Rev.* **67**, 351 (1945).
- ²²G. Herzer, *IEEE Trans. Magn.* **26**, 1397 (1990).
- ²³G. Herzer, *Phys. Scr.*, T **149A**, 307 (1993).
- ²⁴Y.-P. Zhao, R. M. Gamache, G.-C. Wang, and T.-M. Lu, *J. Appl. Phys.* **89**, 1325 (2001).
- ²⁵R. M. Bozorth, *Ferromagnetism* (D. Van Nostrand, Princeton, N.J., 1951), Chap. 18, p. 831.